RSC Advances

ROYAL SOCIETY OF CHEMISTRY

www.rsc.org/advances

Journal Name

ARTICLE

Electrocatalysis by H_2-O_2 Membrane-free Fuel Cell Enzymes in Aqueous Microenvironments Confined by an Ionic Liquid

Received 00th January 20xx,
Accepted 00th January 20xx

DOI: 10.1039/x0xx00000x

www.rsc.org/

Yiduo Wang, Thomas F. Esterle and Fraser A. Armstrong*

An O_2-tolerant [NiFe] hydrogenase and a blue Cu oxidase exhibit excellent catalytic electrochemistry under almost dry conditions – inspiring the concept of a new type of miniature fuel cell able to provide a potential difference close to one volt. Each enzyme is immobilized on a carbon electrode that contacts an aqueous microvolume (1 µL) surrounded by an immiscible, aprotic ionic liquid. Separately, the enzymes display excellent electrocatalytic activity: brought together at a synaptic junction, an anode and cathode modified with each enzyme constitute a membrane-less fuel cell that produces over 0.8 V when equilibrated with a 96 % H_2- 4 % O_2 mixture. The results show there is considerable scope for using ionic liquids to miniaturize selective enzyme fuel cells.

Introduction

Enzymes are inspirational alternatives for precious metal catalysts in specialised fuel cells because they have the merits of high turnover rate per active site, high substrate-selectivity, availability from abundant raw materials and ability to operate under ambient conditions at low overpotentials. The insight that enzymes provide with regard to understanding electrocatalytic mechanism can more than compensate for the practical limitations due to size and stability. Unlike conventional catalysts that lack strong specificity, enzymes allow fuel cells to be miniaturized – operating on a mixed fuel-oxidant feed without a membrane separating the fuel and oxidant [1]. One such enzyme, hydrogenase-1 from *E. coli* (Hyd-1), catalyses H_2 oxidation with a high turnover frequency at moderate driving potentials in the presence of O_2 [2]. Hydrogenase-1 is easily isolated from a common organism, making it very suitable for developing an enzyme-based hydrogen fuel cell [3-5]. Another enzyme, bilirubin oxidase (BOD), is commercially available, highly active and catalyses the four-electron O_2 reduction reaction under mild pH conditions at a smaller overpotential than platinum [6]. Consequently, Hyd-1 and BOD are being exploited as anode and cathode catalysts respectively, in studies of enzymatic H_2-O_2 fuel cells [7-9].

Room temperature ionic liquids (RTILs) are non-volatile, conductive, thermally stable and have wide electrochemical windows, allowing them to be competent electrolytes in fuel cells [10]. Recently an experiment was described in which BOD was shown to be electrochemically active when enclosed with a small amount of water in such a RTIL shell [11]. Experiments with a hydrogenase and RTIL confirmed further that water was essential for activity with these enzymes [12]. In the quest to establish if a H_2/O_2 fuel cell could be miniaturized along similar lines to that achieved with other enzyme fuel cells [13-15], a logical step forward is to incorporate RTILs into new designs. The concepts illustrated in Figure 1 represent development of synaptic membraneless fuel cells that use RTILs to entrap and protect an aqueous microvolume that contains dissolved H_2 and O_2. In these synaptic fuel cells, an anode modified with Hyd-1 and a cathode modified with BOD are brought very close together and electrically connected by a thin gap of water or RTIL (hence, a 'synapse') as depicted in Figure 1 C. In the experiments we now describe, we have used the water-immiscible, hydrophobic RTIL: 1-ethyl-3-methyl-imidazolium-bis(trifluoromethylsulfonyl)imide (EMIMTFSI) (**1**). The viscosity of EMIMTFSI (26.28 cp at 30 ˚C) is about 30 times greater than water (0.798 cp at 30 ˚C), thus providing a good level of mechanical stability.

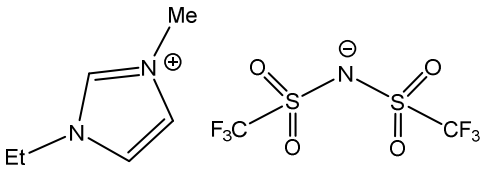

1

Materials and Methods

Hydrogenase-1 was isolated from *Escherichia coli*, as described previously [3]. Bilirubin oxidase (*Myrothecium verrucaria*) was obtained from the Amano company, Japan, and purified further by hydrophobic interaction chromatography with a HiTrap Phenyl HP hydrophobic column (GE Healthcare) [7]. Stock solutions of Hyd-1 (approximately 1 mg mL^{-1}) and BOD (approximately 12 mg mL^{-1}) in phosphate buffer (0.10 M, pH 6.2 at 30 ˚C) were prepared from the as-

[a] Department of Chemistry, Inorganic Chemistry Laboratory, South Parks Road, Oxford OX1 3QR, UK. E-mail: fraser.armstrong@chem.ox.ac.uk

† Footnotes relating to the title and/or authors should appear here.
Electronic Supplementary Information (ESI) available: [details of any supplementary information available should be included here]. See DOI: 10.1039/x0xx00000x

purified enzymes by buffer exchange through four repeated cycles of centrifugation (8161 × g, 5 min), using Centrifugal Filter Devices 50 K (Amicon™ Ultra) at 4 ˚C.

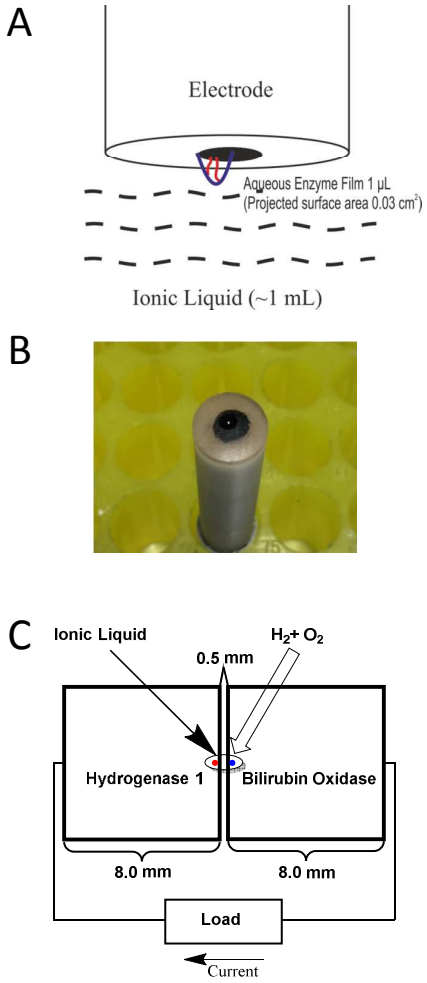

Fig. 1 (A) Scheme showing an electrode modified with an enzyme film (hydrated with approx. 1 µL of buffer) and immersed in water-immiscible ionic liquid. (B) Photograph of the MWNT/PGE electrode on which is deposited 1 µL of aqueous enzyme solution. (C) Diagram of the fuel cell. Two electrodes modified with Hyd-1 (anode) and BOD (cathode) respectively are separated by a gap of 0.5 mm. In all cases the enzyme films are hydrated with a minuscule amount of aqueous buffer. The two electrodes are connected by an aqueous or RTIL synapse.

The RTIL 1-Ethyl-3-methylimidazolium bis(trifluoromethyl-sulfonyl)imide (EMIMTFSI, > 99%) was obtained from Iolitec and heated at 100 ˚C under vacuum for 24 h before use. Toray carbon paper (PTFE treated) was obtained from Alfa Aesar. Multi-walled carbon nanotubes (MWNTs, carbon > 95 %, produced by catalytic chemical vapour deposition, in powder form, outer diameter 6-9 nm, inner diameter 5.5 nm (mode), 6.6 nm (median), length 5 µm) were obtained from Sigma-Aldrich and used as received. Dithiothreitol was obtained from Melford and decamethylferrocene (DmFc) was purchased from Sigma-Aldrich. Adhesive copper tape (0.04 mm thick, 9.52 mm wide, as received: resistance 0.005 Ω through adhesive) and P400 sandpaper were obtained from RS Components. All water used for electrochemical experiments was purified by reverse osmosis and ion exchange to a resistivity of 18.2 MΩ cm at 25 ˚C using a Milli-Q water purification system. The pH of all solutions used for electrochemical studies was determined at the temperature used for measurements. Pyrolytic graphite 'edge' (PGE) disk electrodes (geometric area of graphite: 0.03 cm^2) were constructed from pyrolytic graphite blocks (Momentive Performance Materials Ltd.) as described previously [16]. A dispersion of MWNTs (2.5 mg mL^{-1}) in dimethyl formamide (DMF) was achieved by ultrasonication for 2 h at room temperature. Technical grade H_2 and O_2 were supplied from compressed gas cylinders (British Oxygen Company). The H_2/O_2 mixture ratios were controlled precisely by mass-flow controllers (Sierra Instruments). All other chemicals and solvents were of analytical grade. Phosphate buffer (0.10 M pH 6.2 at 30 ˚C) was prepared by mixing 0.10 M solutions of monosodium phosphate (Fisher) and disodium phosphate (Fisher) at 30 ˚C.

Voltammograms were recorded with Autolab PGSTAT 10 or 20 workstations controlled by NOVA software (version 1.10). Most anaerobic experiments were carried out in a glove box filled with N_2 (O_2 < 4 ppm). The all-glass electrochemical cell consisting of a main compartment and a sidearm has been described previously [7]. The main compartment, which was thermostated with a water jacket, housed the working electrode, the platinum wire counter electrode (7 cm), and a needle to pass gases into EMIMTFSI (volume approximately 1 mL). The sidearm compartment, linked to the main compartment via a Luggin capillary, was filled with EMIMTFSI and contained a Pt wire as quasi-reference electrode (15 cm). Water was excluded, apart from the small area on the electrodes at which enzyme was applied. To supplement the Pt quasi-reference electrode, DmFc (2 mM) was dissolved in the EMIMTFSI to serve as internal reference against which certain potential markers could be calibrated. The $DmFc^{+/0}$ redox couple is widely recognised as a stable reference couple in organic solvents [17, 18] and the lower solubility (of both oxidised and reduced forms) in water helps to minimize possible electron mediation with the electrocatalysts (i.e. Hyd-1 and BOD) contained in the aqueous phase. In addition, the $DmFc^{+/0}$ redox couple is stable in air, in contrast to $Fc^{+/0}$ [19]. All cyclic voltammograms were calibrated against the reversible formal potential, $E_f°$ ($E_f° = (E_p^{red}+E_p^{ox})/2$ where E_p^{red} and E_p^{ox} are reduction and oxidation peak potentials, respectively). Before each experiment, the EMIMTFSI was saturated with substrate gases by bubbling into the liquid.

In a typical voltammetric experiment, the PGE electrode was sanded with P400 sandpaper, then rinsed and sonicated in purified water for 30 min. The electrode was then modified by drop casting 5 µL of MWNT dispersion (2.5 mg mL^{-1} in DMF). The coating was left to dry for 1 hour before depositing a 1 µL aliquot of the Hyd-1 or the BOD stock solution, applied so that only approximately 25% of the MWNT film was covered, the

remaining area being dry. For BOD, this operation was carried out under aerobic conditions on the bench. The BOD film was left to stabilize on the electrode for 1 min, before the electrode was transferred to the electrochemical cell containing a 2 mM solution of DmFc in dry EMIMTFSI. For Hyd-1, the operation was more complicated: prior to spotting onto the electrode, the Hyd-1 was first activated by flowing H_2 above the solution for 30 min in an enclosed vessel held within an anaerobic glove box filled with N_2. Then 1 µL of the activated Hyd-1 solution was pipetted onto the MWNT/PGE electrode. After 1 minute the electrode was transferred to the electrochemical cell containing 2 mM DmFc in EMIMTFSI. For electrochemical experiments carried out under 100% H_2, the entire operation with Hyd-1 was undertaken in the glove box, whereas for experiments carried out under 96% H_2–4% O_2, the electrochemistry was recorded on the bench, as for BOD.

To construct the synaptic fuel cells, two identical pieces of Toray carbon paper modified with MWNTs, were prepared by pipetting 10 µL of MWNT dispersion (2.5 mg mL^{-1} in DMF) onto the middle of one side of a piece of carbon paper measuring 8.0 × 8.0 mm. In each case, the MWNT dispersion was left to dry for 1 h to form a circular MWNT film (diameter ≈ 2.0 mm). Half of the other side of each piece of carbon paper was then attached to a piece of adhesive copper tape (4.0 × 8.0 mm) and thus to copper wire. The two electrodes were then placed on a microscope slide using double-sided tape so that there was a gap of 0.5 mm between the carbon surfaces on each side. The microscope slide was attached to the bottom of a small plastic 'sandwich box' (2L capacity; 14 × 14 × 5.5 cm). Two needles were inserted into the centre of the lid to enable gas mixture to enter and exit, and wires from each electrode exited the box through two very small holes.

The assembly was then transferred to an anaerobic glove box and enzymes were applied by pipetting 2 µL aliquots of activated Hyd-1 and BOD stock solution, respectively, onto the MWNT-modified carbon surfaces of anode and cathode. The enzyme deposits on both electrodes, (diameter approximately 1 mm in each case) were left to dry for 15 minutes in the anaerobic glove box atmosphere. This drying step is crucial to prevent Hyd-1 and BOD films from crossing the synapse and mixing with each other. Meanwhile, on the bench, 1 mL volumes of water and EMIMTFSI were saturated with 96 % H_2–4 % O_2 by bubbling the gas mixture through for 0.5 h.

The enzyme-loaded fuel cell was moved back to the bench to complete the construction. In one case the dry Hyd-1 and BOD films on the two electrodes were hydrated by pipetting 1 µL of the gas-equilibrated water onto each spot and another 1 µL of water across the synaptic gap. Each of the two aqueous enzyme films was then coated with 1 µL of EMIMTFSI and the synaptic gap that was already connected by 1 µL of water was coated with a further 1 µL of EMIMTFSI, hence sealing a continuous aqueous phase. In the second case, the Hyd-1 and BOD films on the electrodes were rehydrated with two separate 1 µL aliquots of water then each droplet was coated with 2 µL of EMIMTFSI, and finally, a further 2 µL of the same EMIMTFSI was applied to fill the 0.5 mm synaptic gap between the two electrodes.

Within 1 min after construction, the box was sealed and the fuel cells were connected to the Autolab PGSTAT 20. A 96 % H_2–4 % O_2 mixture was then supplied via the entry and exit needles on the lid. The temperature was 26 ± 2 ˚C. At the start of each experiment, chronopotentiometry at zero current was carried out to establish the open (maximum) circuit voltage (OCV) of the fuel cell. Power curves describing the relationship between power and cell voltage were obtained by linear scan voltammetry starting from the OCV to 0 V, at the low scan rate of 1 mVs^{-1} [20]. The corresponding power (P) at each voltage was calculated from the equation $P = V \times I$. The power was divided by the total electrode area (0.0157 cm^2) to obtain the practical power density which was plotted against V to obtain power curves.

Results and Discussion

Figure 2 shows successive cyclic voltammograms obtained for H_2 oxidation by Hyd-1 adsorbed from a 1 µL H_2-saturated aqueous droplet (pH 6.2, 0.10 M phosphate) deposited at a small area of the MWNT/PGE electrode which then was placed in EMIMTFSI. Hydrogen gas was passed through the cell headspace without bubbling into the ionic liquid, in order to minimise disruption of the aqueous environment around the enzymes. Cyclic voltammograms were then recorded, as shown in Figure 2, correcting the potential scale at each cycle against the $DmFc^{+/0}$ redox couple that is essentially confined to the EMIMTFSI phase. A stable cyclic voltammogram of the MWNT/PGE electrode in the absence of enzymes and the aqueous phase is also shown. The voltammograms show a sharp peak at approximately -0.15 V vs $DmFc^{+/0}$, due to enzymatic H_2 oxidation occurring in the aqueous phase. Upon successive cycles, the signal diminishes in size and the onset of H_2 oxidation shifts to more positive potential, consistent with the aqueous phase gradually becoming more acidic [21].

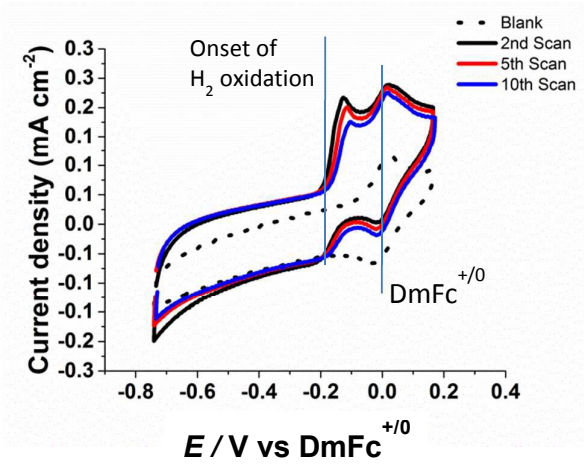

Fig. 2 Cyclic voltammetric scans showing catalytic H_2 oxidation by Hyd-1 adsorbed at a MWNT/PGE electrode and contacting 1 µL of 0.1 M phosphate buffer (pH 6.2). For electrical contact, the aqueous microenvironment is surrounded by EMIMTFSI (approximately 1 mL) containing 2 mM DmFc and saturated with 1 bar H_2. Black, red and blue solid lines represent the 2nd, 5th and 10th scans respectively. Temperature 30 ˚C, scan rate 10 mV s^{-1}. The control experiment ('blank') with DmFc but no enzyme is shown as a dotted line.

The catalytic activity of the enzyme observed by cyclic voltammetry was made possible due to an aqueous pocket surrounding the enzyme to separate the RTIL from the protein

surface and thus ensure an active enzyme. The aqueous environment is absolutely essential for catalysis: experiments conducted after allowing the aqueous droplet to dry naturally for 15-20 minutes showed no catalytic wave due to H_2 oxidation. However, the enzyme was not degraded by dehydration because addition of a microdrop of water (1 µL) onto the electrode resulted in almost full recovery of electrocatalytic activity. The lack of hydrogenase activity in pure RTIL is consistent with observations reported by Ciaccafava *et al* [12].

Figure 3 shows analogous experiments to investigate electrocatalytic O_2 reduction by BOD in the same confined aqueous microenvironment. The BOD was applied as a 1 µL droplet of air-saturated 0.10 M phosphate buffer, pH 6.2, to part of the electrode surface. After 1 minute, the electrode was placed into the electrochemical cell containing EMIMTFSI saturated with 1 bar O_2. Oxygen was passed through the cell headspace without bubbling into the ionic liquid, to avoid disturbing the aqueous layer around the enzyme molecules. The cyclic voltammograms show a strong catalytic wave due to O_2 reduction that commences at about +0.9 V vs $DmFc^{+/0}$; in contrast the enzyme-free MWNT/PGE electrode under the same conditions shows only the peaks due to the $DmFc^{+/0}$ redox couple. The O_2 reduction catalytic wave decreases in amplitude upon successive cycles and shifts to more negative potential, the onset occurring at approximately +0.7 V on the 4th scan. This shift is as expected for a local increase in pH due to proton consumption [6].

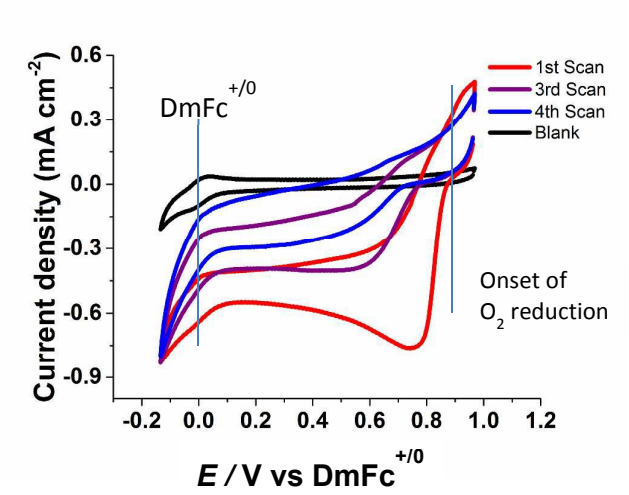

Fig. 3 Continuous cyclic voltammograms of catalytic O_2 reduction by BOD adsorbed at an MWNT/PGE electrode and contacting 1 µL of 0.10M phosphate buffer (pH 6.2). For electrical contact, the aqueous microenvironment is surrounded by EMIMTFSI (approximately 1 mL) containing 2 mM DmFc and saturated with 1 bar O_2. Red, purple and blue solid lines represent the 1st, 3rd and 4th scans, respectively. Black solid line: blank MWNT/PGE electrode. Temperature 30 ˚C, scan rate 10 mV s^{-1}. The control experiment ('blank') with DmFc but no enzyme is shown as dotted line.

Figure 4 shows catalytic voltammograms of Hyd-1 and BOD each measured under a non-explosive, H_2-rich aerobic atmosphere. In each case the enzyme was adsorbed on a MWNT/PGE electrode, then entrapped within a 1 µL aqueous droplet (0.10 M phosphate, pH 6.2, equilibrated with 96 % H_2- 4 % O_2) and immersed in EMIMTFSI also equilibrated with 96 % H_2- 4 % O_2 at 30 ˚C. The blank MWNT/PGE electrode shows only direct, non-enzymatic reduction of O_2 at a potential below -0.19 V vs $DmFc^{+/0}$. For Hyd-1, the non-enzymatic O_2 reduction commences close to the potential for the enzyme-catalysed H_2 oxidation, and the actual onset potential for H_2 oxidation is obscured. For electrocatalytic O_2 reduction by BOD, a sharp peak is observed at +0.89 V vs $DmFc^{+/0}$ and the onset potential is close to + 1 V. The onset potentials measured under these H_2-O_2 fuel cell conditions indicate that an open-circuit voltage close to 1 V should be achievable.

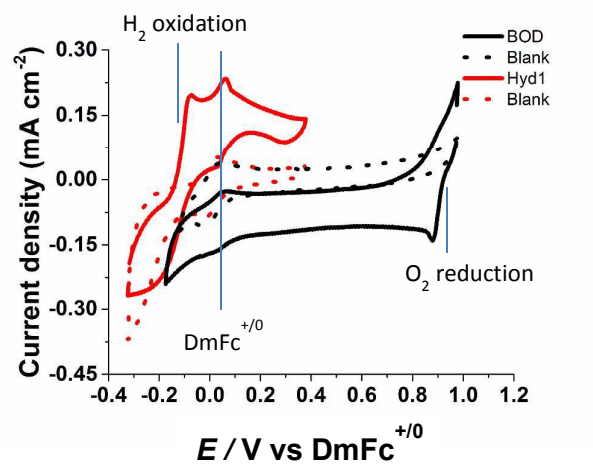

Fig. 4 Cyclic voltammograms (current density, first scans) of H_2 oxidation by Hyd-1 (red solid line) and O_2 reduction by BOD (black solid line) each attached to an electrode as for Figs 2 and 3. Voltammograms of blank MWNT/PGE electrodes are shown as dashed lines. Surrounding EMIMTFSI contains 2 mM DmFc and is saturated with 96 % H_2 - 4 % O_2 (v/v) at 30 ˚C. Scan rate 10 mV s^{-1}.

A common feature of the continuous cyclic voltammetric experiments was that the electrocatalytic activities of both Hyd-1 and BOD diminish with time. (Referee 1. Q2) However, even when the activities had become negligible, catalytic activity was still observed when the electrode was transferred to aqueous buffer saturated with either H_2 or O_2, respectively. We also established that EMIMTFSI showed no difference in behaviour after prolonged exposure to H_2 oxidation and O_2 reduction for at least 4 weeks.

The definitive experiments were carried out using the synaptic fuel cell shown in Figure 5 A, constructed as described in Materials and Methods. The synapse between two electrodes was either a direct aqueous connection or one provided by the ionic liquid. Because the fuel cell operates under a very small flow rate of gases through the box, the gas flow did not disturb the connection.

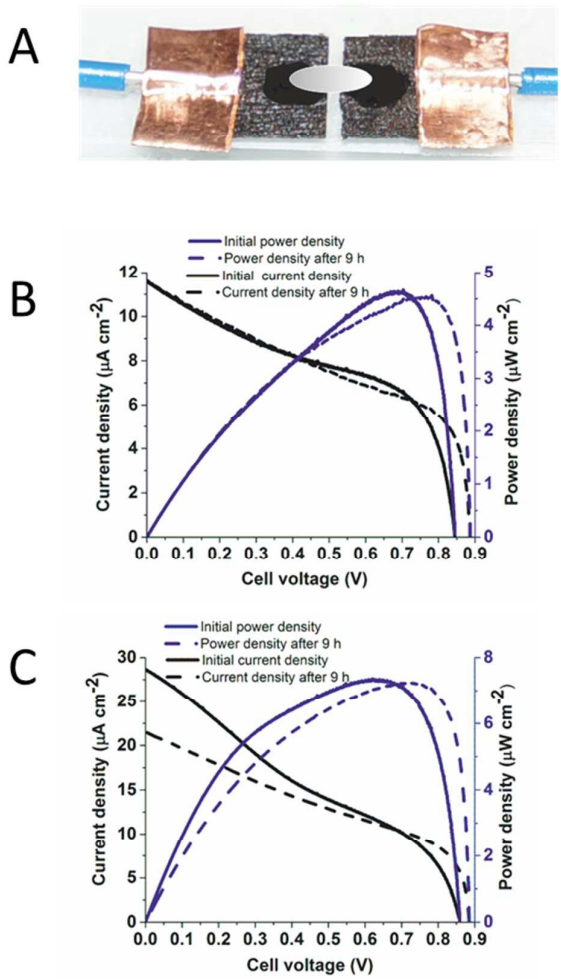

Fig. 5 (A) The synaptic fuel cell assembly. Black areas correspond to aqueous zones where enzymes have been spotted on the electrodes and the pale grey area indicates the protective coverage of EMIMTFSI over the two electrodes. (B and C) Performances of the fuel cells, 26 ± 2 ˚C, box atmosphere 96 % H_2 - 4 % O_2. Solid lines show initial polarisation curve (black) and power curve (blue). Dashed lines show polarisation curve (black) and power curve (blue) of the fuel cells after 9 h's operation under at 0.75 V. Panel B shows results for two electrodes linked by synaptic aqueous phase and RTIL coating. Panel C shows results for two electrodes linked by ionic liquid alone.

Figure 5 B shows the polarisation and power curves of the fuel cell with the two electrodes linked directly by the aqueous synapse as well as the RTIL coating. This fuel cell provided an initial OCV of 0.85 V, climbing to 0.89 V, with a maximum power density (4.5 μW cm^{-2}) close to 0.8 V once a steady reading was established. The small increase in OCV probably reflects activation of some Hyd-1 that had undergone inactivation during exposure to air in the last stage of construction, and possibly a decrease in interference from non-catalytic O_2 reduction at the Hyd-1 'anode' which is more marked in freshly prepared electrodes. Figure 5 C shows the polarisation and power curves of the fuel cell with separate aqueous film electrodes linked only by ionic liquid under 96 % H_2 - 4 % O_2. This fuel cell provided an initial OCV of 0.86 V, climbing to 0.89 V, with a maximum power density (7.3 μW cm^{-2}) close to 0.75 V upon stabilisation. The stability of the synaptic fuel contrasts with the individual cyclic voltammetry experiments, the most likely reasons being that the exchange of gases with the aqueous electrolyte is at steady state with respect to the rate of consumption, the fuel cell reaction is pH-neutral, and the rate of H^+ transfer between the two electrodes is adequate even when the direct aqueous connection is replaced by ionic liquid.[8, 9] The robust similarity regardless of whether the two aqueous zones are merged into one across the synapse suggests that water molecules in the aqueous enzyme shells can easily move into the EMIMTFSI to serve as the proton carrier, although H(2) at $EMIM^+$ cation is weakly acidic [22, 23] and EMIMTFSI may be directly active in proton transport [24].

In summary, we have demonstrated the scope for enzymatic fuel cells that can be miniaturized by using an ionic liquid to trap the enzymes within aqueous microenvironments. Both fuel cell enzymes, Hyd-1 and BOD, are highly active in an limited amount of water contained within a shell of water-immiscible EMIMTFSI. The synaptic enzymatic H_2–O_2 fuel cell uses a much smaller volume of electrolyte (approximately 6 μL) than previous enzymatic H_2-O_2 fuel cells (> 1 mL) [7, 8, 25]. The OCV and optimal potentials of the synaptic fuel cell, nearly 0.9 V and close to 0.8 V respectively, compare well with the thermodynamic reversible value of 1.23 V at 25 ˚C. The results help highlight the possibilities for enzymes operating under limited aqueous conditions with the aid of ionic liquids as conductive media.

Acknowledgements

We are grateful to Elena Nomerotskaia for assistance with enzyme purification and Luke Shoham for undertaking some preliminary experiments. We thank the Engineering and Physical Sciences Research Council (EP/H019480/1; Supergen V) for financial support. F.A.A. is a Royal Society-Wolfson Research Merit Award holder.

Notes and references

1. J. A. Cracknell, K. A. Vincent and F. A. Armstrong, *Chem Rev*, 2008, **108**, 2439-2461.
2. R. M. Evans, A. Parkin, M. M. Roessler, B. J. Murphy, H. Adamson, M. J. Lukey, F. Sargent, A. Volbeda, J. C. Fontecilla-Camps and F. A. Armstrong, *J Am Chem Soc*, 2013, **135**, 2694-2707.
3. M. J. Lukey, A. Parkin, M. M. Roessler, B. J. Murphy, J. Harmer, T. Palmer, F. Sargent and F. A. Armstrong, *Journal of Biological Chemistry*, 2010, **285**, 3928-3938.
4. M. J. Lukey, M. M. Roessler, A. Parkin, R. M. Evans, R. A. Davies, O. Lenz, B. Friedrich, F. Sargent and F. A. Armstrong, *J Am Chem Soc*, 2011, **133**, 16881-16892.
5. K. A. Vincent, A. Parkin and F. A. Armstrong, *Chem Rev*, 2007, **107**, 4366-4413.
6. L. dos Santos, V. Climent, C. F. Blanford and F. A. Armstrong, *Phys Chem Chem Phys*, 2010, **12**, 13962-13974.
7. A. F. Wait, A. Parkin, G. M. Morley, L. dos Santos and F. A. Armstrong, *J. Phys. Chem. C*, 2010, **114**, 12003-12009.

8. S. Krishnan and F. A. Armstrong, *Chem Sci*, 2012, **3**, 1015-1023.
9. L. Xu and F. A. Armstrong, *Energy & Environmental Science*, 2013, **6**, 2166.
10. T. Welton, *Chem Rev*, 1999, **99**, 2071-2083.
11. J. Kuwahara, R. Ikari, K. Murata, N. Nakamura and H. Ohno, *Catal Today*, 2013, **200**, 49-53.
12. A. Ciaccafava, M. Alberola, S. Hameury, P. Infossi, M. T. Giudici-Orticoni and E. Lojou, *Electrochim Acta*, 2011, **56**, 3359-3368.
13. T. Chen, S. C. Barton, G. Binyamin, Z. Q. Gao, Y. C. Zhang, H. H. Kim and A. Heller, *J Am Chem Soc*, 2001, **123**, 8630-8631.
14. N. Mano, F. Mao and A. Heller, *J Am Chem Soc*, 2002, **124**, 12962-12963.
15. H. H. Kim, N. Mano, X. C. Zhang and A. Heller, *Journal of Electrochem Society*, 2003, **150**, A209-A213.
16. R. M. Evans and F. A. Armstrong, *Methods in molecular biology*, 2014, **1122**, 73-94.
17. A. A. J. Torriero, J. Sunarso and P. C. Howlett, *Electrochim Acta*, 2012, **82**, 60-68.
18. I. Noviandri, K. N. Brown, D. S. Fleming, P. T. Gulyas, P. A. Lay, A. F. Masters and L. Phillips, *The Journal of Physical Chemitry B*, 1999, **103**, 6713-6722.
19. J. K. Bashkin and P. J. Kinlen, *Inorg Chem*, 1990, **29**, 4507-4509.
20. V. J. Watson and B. E. Logan, *Electrochem Commun*, 2011, **13**, 54-56.
21. B. J. Murphy, F. Sargent and F. A. Armstrong, *Energy & Environmental Science*, 2014, **7**, 1426-1433.
22. P. Bonhôte, A.-P. Dias, N. Papageorgiou, K. Kalyanasundaram and M. Grätzel, *Inorg Chem*, 1996, **35**, 1168-1178.
23. T. Koddermann, C. Wertz, A. Heintz and R. Ludwig, *Chemphyschem*, 2006, **7**, 1944-1949.
24. K. D. Kreuer, *Chem Mater*, 1996, **8**, 610-641.
25. S. Zhang, N. Sun, X. He, X. Lu and X. Zhang, *Journal of Physical and Chemical Reference Data*, 2006, **35**, 1475.

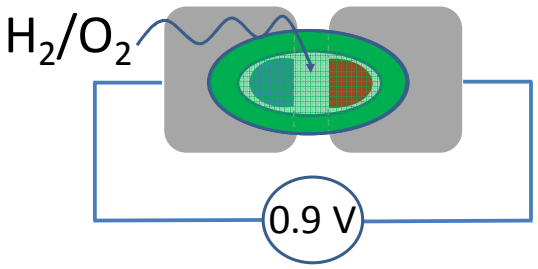

A synaptic enzyme fuel cell comprising ‘wet’ hydrogenase and bilirubin oxidase electrodes enclosed in shell of ionic liquid.